

2.3 Analysis of experimental observations with the 2D model

2.3.1 Short-term preservation of IRBCs. Adjustment of INDISIM-RBC.

The reproduction of the first short-term culture of malaria infected RBCs *in vitro* was used to check the relevant parameters to set the calibration of the program. The reference employed is the experiment of Pavanand et al. (1974) for preserving *P. falciparum* in culture for more than a complete cycle of infection. Infected RBCs are maintained in static cultures for 64 hours with effective parasite proliferation. Cultures of 0.2 ml are incubated at 37°C in a mixture of culturing medium and human sera, with no medium renewal. Concentration of the hematocrit is 9.36% in volume. Size of the culturing aliquots and shape of the hematocrit layer is not specified. The initial glucose concentration is 2g/l and initial lactate concentration is 0 (Diggs et al., 1971). Initial parasitaemia is approximately 1%. The experimental measurements are parasite counts per 1000 RBCs. Three forms of the are distinguished by their infection stages: rings, trophozoites and schizonts. No distinction is made between schizonts and fragmenters.

The experimental data regarding the parasite counts of each of the infection stages ($0, R, T$ and $S + F$) are used to build and calibrate the model. The initial parasitaemia $\%I_0$ can be inferred from the experimental data assuming no accidental death rates for the healthy RBCs and Ring stage forms. The values for the probability of accidental death per time step and infection stage $P_{death}(0, R, T, S \text{ and } F)$, the maximum susceptibility to invasion of healthy RBCs P_{max} and the initial post-invasion time distribution for IRBCs are set to adjust experimental data (post-invasion times are uniformly distributed from 1 to a maximum initial post-invasion time).

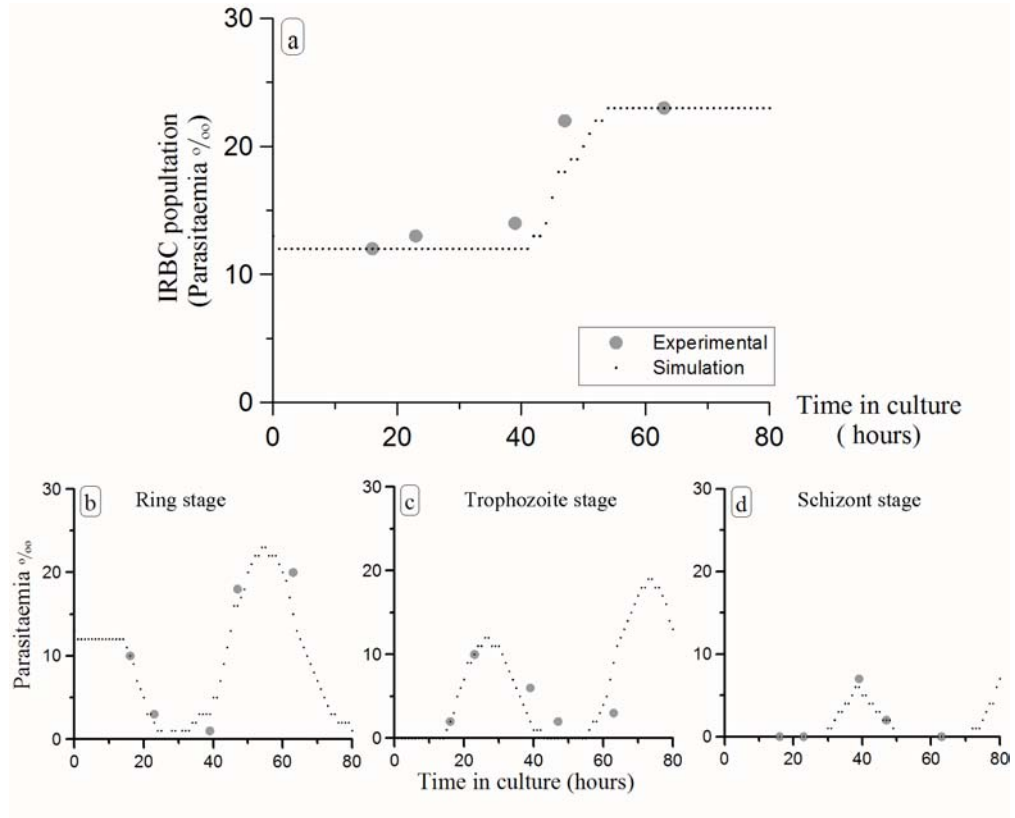


Figure 2.5: *Reproduction of the experimental results for short-term in vitro preservation of *P. falciparum* (Pavanand et al., 1974) with the version 2Dv.1. Grey dots represent experimental results. Black small dots represent simulation results. The statistical variance is not shown. a) Total parasite count. b) Ring-stage IRBCs. c) Trophozoite-stage IRBCs. d) IRBCs at schizont and fragmenter stage.*

Simulation results obtained with version 2Dv.1 are shown in Figure 2.5. Results obtained with version 2Dv.2 with the same input parameter sets (with the values of P_{death} and $P_{prop} = 0.05$ readjusted in accordance to the modification of the time step) do not show significant differences.

The variance of the model is assessed performing 100 repetitions of the simulations with a fixed set of parameters and varying the random seed. It has been found that, once every parameter is fixed, simulations are highly determined, and the variance is $\sigma^2 < 10^{-3}$.

The comparison of the model outcome with experimental measurements is usually

carried out qualitatively because the use of statistical tests can be deceptive and must be handled with care. For instance, a Student's t-test suggest that both data sets are not significantly different ($p - value = 0.08$), but the Kolmogorov-Smirnov test gives only a non-significative probability that both samples come from the same distribution function ($r^2 = 0.7143$). For an outlined description of the statistical tools appropriate to compare each set of samples see Appendix C.

Input parameter	Value			
$\%I_0$	0.12%			
$P_{death}(-)$	0	R	T	$S + F$
	0	0	0.005	0.025
P_{max}, P_{min}	0.8 , 0			
$t_{INF}^{MAX}(t = 0)$	4 <i>ts</i>			

Table 2.3: Values for some initialization parameters in the *2Dv.1* simulations of the experiments for short -term *in vitro* presevation of *P. falciparum* (Pavanand et al., 1974). Measured initial parasitaemia ($\%I_0$), and values set to best fit experimental outcome: probability of accidental death per time step and infection stage ($P_{death}(0, R, T, S$ and $F)$), maximum susceptibility to invasion of healthy RBCs (P_{max}) and maximum value of the post-invasion time of the inoculated IRBCs ($t_{INF}^{MAX}(t = 0)$).

The values for the input parameters have been searched through the systematic and oriented trial of different set of values (Prats, 2008). The values that best fit the experimental observations are outlined in Table 2.3. The sensibility of the model to slight modifications on the values of the parameters has been qualitatively assessed. For instance:

1. the increase in parasitaemia (or growth ratio GR) is more affected by variations in the accidental mortality rate P_{death} than by those in the infection probability P_{max} . In fact, varying P_{max} from 0.7 to 1 does not significantly alter the simulations outcome, while small modifications of $P_{death}(S + F)$ from 0.25 to 0.255 make a substantial difference.
2. The initial distribution of post-invasion times is determinant to the best fit to the experimental data on the parasite counts of the different stages of IRBCs. The best-fit function is a uniform distribution of post-invasion times truncated for post invasion times greater than $t_{INF}^{MAX}(t = 0)$.

The analysis of sensibility of input parameters is not exhaustive. The model outcome could be more accurately fitted to the experimental observations, yet the current qualitative fitting of the model indicates that the modeled infection dynamics and the structure

of the post-invasion times among IRBCs are consistent with the observations of real cultures.

A thorough assessment of the sensibility of parameters is important for well-established models, in order to improve their predictive capability. Models with less parameters and a simpler structure are more suitable for such a use. A discussion on the role of different kinds of models is put forward in Section 4.2.

2.3.2 Long-term cultivation of IRBCs. Readjustment of INDISIM-IRBC.

The experiment carried out by Trager and Jensen (1976) is used to validate the qualitative behaviour of the model when simulating cultures with multiple cycles of infection. Healthy and infected RBCs are maintained in static cultures for several weeks with effective parasite proliferation. Cultures of 1 ml with 5% hematocrit are incubated at 38°C under a low-oxygen atmosphere and culturing conditions referred in Table 1.2, in flat bottomed vials. The depth of the hematocrit layer (*HLD*) is set to a value $HLD \sim 0.1$ mm. Initial concentrations of glucose and lactate are 2.667 mM and 0 mM, respectively.

Subcultivations are performed every three or four days, depending on the parasitaemia. Variable dilutions are effected to obtain a parasitaemia around 0.5% after subculture. In particular, the dilution factor of the sample to the subculture is 3-fold, 3.5-fold or 4-fold, the later being the most usual. Some of the subculturing are indicated in the experiment, while others are not specified but may be inferred from the indicated dilution shown in the experimental data sets. Four forms of the asexual intraerythrocytic stages of the parasite are distinguished in this experiment (*0, R, T, S and F*).

Two different protocols are presented: the *continuous method* and the *candle-jar method*. The first one, IRBCs are maintained for 48 days out from a inoculum with $\%I_0 = 0.32$ in a semiopen system with a continuous flow of culture medium. Medium renewal is performed continuously at a rate of 50 ml/day out from a reservoir of 120 ml. The second protocol achieves the preservation of parasitized red blood cells for more than three months in a closed culture with discrete daily medium renewal. The medium renewal is carefully executed, so no disturbance of the RBC population is expected and no agitation must be considered due to medium renewal.

Both protocols use the same blood source, parasite strain and culture medium preparation, and maintain the hematocrit under similar geometrical conditions. Two culture lines (lines A and B) are cultured under different atmospheric conditions, B being apparently more suitable for RBC development (Jensen, 1988). At variable time spans, (1-day to 5-day) the culture is sampled and the parasitaemia and age structure are measured.

Both lines are simulated with the same model. The experimental parasite counts of each of the infection stages ($0, R, T, S$ and F) are used to check the capacity of the model of simulating long-term culture systems. The maximum susceptibility to invasion of healthy RBCs P_{max} is common for both trial lines, as they share the parasite strain and the RBC source. Their values are set to best adjust experimental data. The initial parasitaemia $\%I_0$ and the input parameters describing the external manipulations on the system are set according to the specifications of each experimental procedure. The initial post-invasion time distribution for IRBCs (mean value $\bar{t}_{INF}(t=0)$) and the values for the probability of accidental death per time step and infection stage $P_{death}(0, R, T, S$ and $F)$ are set independently for each trial to best fit the experimental data. Every value is determined using the procedure explained in Section 2.3.1. They are presented in Table 2.4.

Noteworthy, the inoculum of line B is much more synchronized than the one of line A (the initial distribution of post invasion times is narrower in line B). This could be explained through a hypothetical rupture of mature parasite forms during the transfer from one culture system to the other.

The only difference between the models of line A and B is that the former has a continuous replacement of part of its culturing medium. This is implemented as the replacement of a fraction of the culture medium at each time step ($f = \frac{50 \text{ ml/day}}{120 \text{ ml}} \cdot \frac{1 \text{ day}}{24 \text{ ts}}$). This replacement entails the removal of extracellular merozoites. Thus, each merozoite has a probability of 0.017 of being removed from the medium.

Input parameter	Line A	Line B
$\%I_0$	0.32%	0.14%
$\bar{t}_{INF}(t=0)$	22 ts	2 ts
$P_{death}(-)$	S F	S F
	0.006 0.01	0.005 0.012
P_{max}, P_{min}	0.85, 0	

Table 2.4: Values for some initialization parameters in the simulations of the experiments for long-term *in vitro* cultivation of *P. falciparum* (Trager and Jensen, 1976). Measured initial parasitaemias ($\%I_0$) and best fit values for mean value of the post-invasion time of the inoculated IRBCs ($\bar{t}_{INF}(t=0)$) and probability of accidental death per time step and infection stage ($P_{death}(S$ and $F)$), for healthy RBCs, Rings and Trophozoites, $P_{death} = 0$) for each line of the culture. Maximum and minimum susceptibility to invasion of healthy RBCs (P_{max}, P_{min}) are common for both lines.

The analysis of the variability and sensibility of the model provide similar results to the ones presented in the last section. Two differences with respect to the previous conclusions

are:

1. in this case, the post-invasion time distributions among inoculated IRBCs that best fit the initial measurements of the age structures are normal distributions around a mean value $\bar{t}_{INF}(t = 0)$ with standard deviation 0.1. The model shows very dissimilar results for different input distributions of the post-invasion times, when multiple consecutive cycles are taken into account.
2. the model is highly sensible to variations on the parameters that regulate the culturing protocols. Small variations on the subcultivation span or dilution factor may lead to significantly different courses of the infection. The experimental subculturing protocols are not described with enough detail. In fact, the moment of external manipulations are not specified and must be deduced from the results.

An increased number of parameters (the initialization parameters presented in Table 2.4 plus the input parameters that describe the external manipulations of the system) now govern the dynamics of the model in a complex and interrelated way. These parameters represent magnitudes or events that can not be directly measured, and must be fixed to better adjust the evolution of the infection and of each of the IRBC stages.

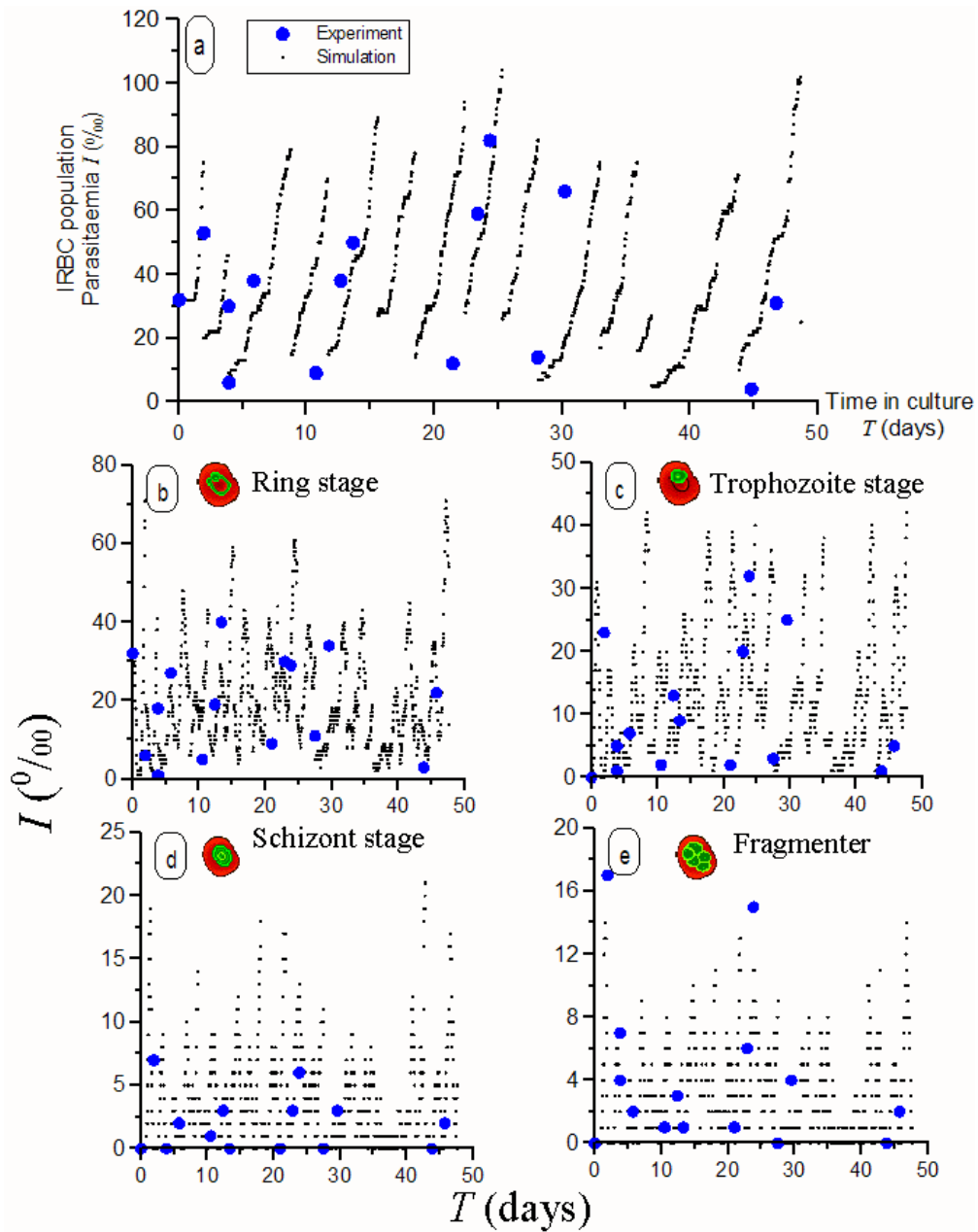


Figure 2.6: Simulation results compared to experimental data of the infection course in the Continuous-flow cultivation (Line A) of *P. falciparum* IRBCs (Jensen and Trager, 1978). Blue dots stand for experimental measurements. Black small dots represent simulation results. Leap in the black dots trail indicate a subcultivation. a) Total parasite count. b) Ring-stage parasite count. c) Trophozoite-stage parasite count. d) Schizont-stage parasite count. e) Fragmenter-stage parasite count.

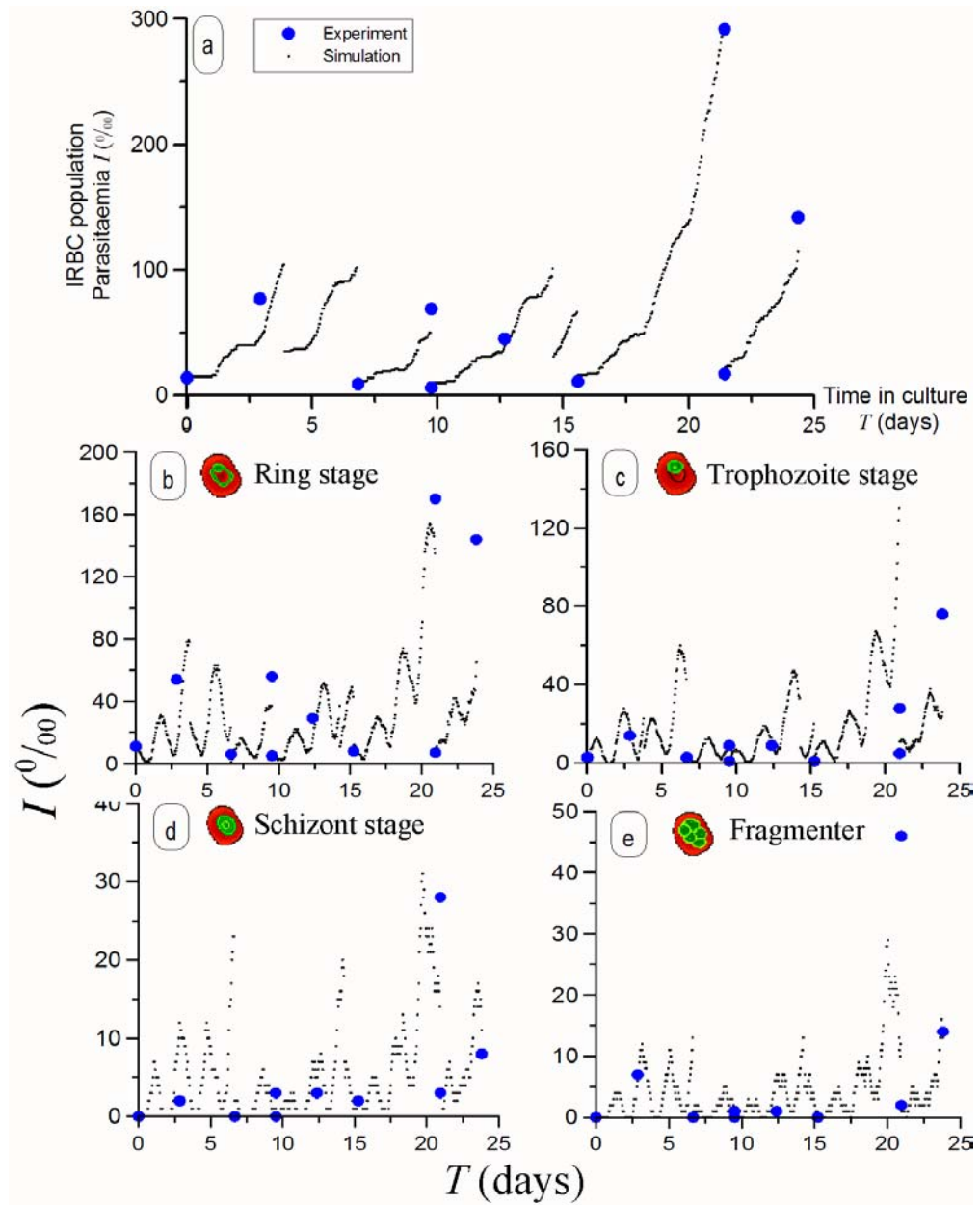


Figure 2.7: Simulation results compared to experimental data of the infection course in the *Candle-jar* cultivation (Line B) of *P. falciparum* IRBCs (Jensen and Trager, 1978). Blue dots stand for experimental measurements. Black small dots represent simulation results. Leap in the black dots trail indicate a subcultivation. a) Total parasite count. b) Ring-stage parasite count. c) Trophozoite-stage parasite count. d) Schizont-stage parasite count. e) Fragmenter-stage parasite count.

The degree of adjustment of the model outcome to the experimental data is assessed through:

1. qualitatively checking the similarity of the temporal evolution of the IRBC population structure (see Figures 2.6 and 2.7, total IRBC evolution and for each of the infection stages); and
2. comparing the average infection growth ratios between two consecutive samplings $\langle GR_{sample} \rangle$ all through the culture (see Table 2.5).

$\langle GR_{sample} \rangle$	Simulation Outcome	Experimental results
Line A	7 ± 3	8 ± 5
Line B	12 ± 6	10 ± 4

Table 2.5: Temporal average growth ratio of the parasitaemia during to consecutive samplings $\langle GR_{sample} \rangle$. They stand for approximately two complete intraerythrocytic cycles of the parasite. Simulation results are consistent with experimental measurements.

Simulation results obtained with version *2Dv.1* are shown in Figure 2.6. Results obtained with an equivalent model in version *2Dv.2* do not show significant differences. The outcome of the model when performing several repetitions of the simulations varying the random seed show highly dissimilar long-term evolutions of the IRBCs population structure, but no significant differences in $\langle GR_{sample} \rangle$.

The comparison between simulated and experimental growth ratios allows concluding that the model is consistent with the system it represents. However, it must be stressed that the uncertainty of GR_{sample} is very high both in experiments and simulations. Again, a more accurate quantitative fit of the simulation outcome to the experimental data would be very toilsome and would not provide much useful information. On the other hand, the qualitative reproduction of the experimental dynamics with the simplest model assumptions provides a certain validation of the model: at least, the model and the experimental cultures behave in a similar way.

2.3.3 Patterns observed in *in vitro* cultures.

The accurate quantitative reproduction of several particular datasets from single experimental trials positively allows extracting some conclusions. First, it indicates that the model includes enough information at an individual level to reproduce the complex observed behaviour. Second, it suggests that the rules in the model are a good representation of the processes occurring in the real culture systems, because the same rules serve

to simulate different cultures. And third, provides an estimation of the values (or at least order of magnitude) of some magnitudes that can not be easily measured (such as the RBC death rate, or the infection probability).

However, it does not provide enough arguments to assess the validity of the model by its own. First, because it can't be disproven that simpler models could also reproduce the observed behaviour. Second, because the coincidence between the model outcome and experimental observations does not ensure that it accounts for *real* underlying mechanisms. And third, because obtaining the "best fit" requires adjusting the values of several parameters simultaneously, and different sets of parameters could provide similar outcomes. The exhaustive exploration of the parameter space would be extremely time-consuming and has been carried out just to a reasonable extent here.

So, what else can be done to assess the validity of the model? The reproduction of a group of independent patterns observed in real culture systems at different scales and regarding distinct phenomena can provide increasing confidence on the capacity of the model to capture the essence of the experiments. If the model reproduces different uncorrelated phenomena and features of the real systems, it means that it correctly represents the reality. Then, the modelled rules can be better regarded as indicators of the essential underlying processes occurring in real cultures. Some independent patterns are reproduced below. A more detailed discussion on the arguments presented in this paragraph may be found in Section 4.1.

Strains of *P. falciparum*

The performance of *in vitro* cultivation of *P. falciparum* strongly depends on the strain, ranging from the unfeasibility of setting cultures to highly effective harvests (Chin and Collins, 1980). The variability in the performance of a fixed strain is also very high and the evolution of observed cultures show that the multiplication ratio of the number of IRBCs per infection cycle does not solely depend on the strain.

The results obtained by Butcher (1982) reflect this intrinsic variability. Three different strains of *P. falciparum* were maintained under static (*candle-jar*) and suspension conditions. The parasite was maintained in continuous cultures with the same blood source and conditions during approximately one month. Renewal of medium was performed daily but was skipped sometimes between two consecutive subcultivations. Samples were extracted when setting new subcultures every three days. The growth ratio (GR_{72}) was then measured. Growth ratios were calculated as the ratio between the observed parasitaemias at the beginning and end of each subculture. The experimental results are presented in table 2.6.

	Strain A		Strain B		Strain C	
	Static	Susp.	Static	Susp.	Static	Susp.
GR_{72} 1	6.9 *	1.8 *	1.8 *	14.4 *	5 *	23.8 *
GR_{72} 2	10.6 *	2.0 *	1	4.5	0.7 *	9.0 *
GR_{72} 3	8.8 *	8.2 *	0	8.0	4.4 *	10.8 *
GR_{72} 4	9.1	11.6	7.1	22.0	6.8 *	9.2 *
GR_{72} 5	7.1	6.0	1.8 *	2.9 *	7.7 *	19.7 *
GR_{72} 6	10.6	16.5	9	25.3	-	-
GR_{72} 7	5.1 *	3.3 *	-	-	-	-
Means	8 ± 2	7 ± 5	3 ± 4	12 ± 9	5 ± 3	14 ± 7

Table 2.6: *Experimental 3-day growth ratios (GR_{72}) for Static (candle-jar culture conditions) and continuously agitated cultures (“Susp.” stands for RBCs in suspension) for 3 different strains of *P. falciparum*. The symbol * indicates that no medium renewal was carried out between two samples. Reprinted from (Butcher, 1982).*

The first remark to the experimental observations is that the intrinsic variability of any real culture system usually allows drawing only tentative conclusions regarding the observed behaviours. The averaged values are often accompanied by such high uncertainties that they can not be stated to be significantly different. Using statistical toolpacks such as ANOVA (a collection of statistical models to perform the ANalysis Of VAriance of datasets, i.e.: Student’s t-test, Kruskal-wallis test, Kolmogorov-Smirnov test, among tothers; see Appendix C) facilitates the discrimination of data, but still it is not enough to distinguish different strains.

Even discriminating between different culturing protocols is controversial. For instance, results from Strains B and C suggest that suspended cultures are more efficient than static cultures but this is not supported by the observations of Strain A. Apart, results from Strains A and B, which combine subcultures with and without medium renewal suggest that the lack of medium replacement hinders the development of the parasite. However, Strain C, whose medium was not renewed in between subcultures shows a qualitatively increased performance.

The simulations of the different set of experiments carried out using INDISIM show similar statistical behaviours and their analysis faces analogous problems. One strategy to follow in order to analyze the model is to focus on the effect of one single parameter, while all the other set of parameters are fixed.

For instance, modifying the strain can be associated to varying the infection capability of the merozoites P_{inf} . Variations in thos parameters used to set P_{inf} , within the ranges $0.7 < P_{max} < 1$, and $0 < P_{min} < P_{max}$ entail fine variations of the simulated outcome growth ratios (GR_{48}). Noteworthy, this small modification of GR_{48} can eventually

lead to high dissimilarities between cultures under similar harvesting protocols, because the effect of consecutive cycles has a nonlinear feedback, and also because the external manipulations of the system are triggered at fixed moments and can affect systems with slightly different configurations in very unlike manners.

An additional remark specifically regarding the effect of varying the probability of invasion in the simulations introduces a different topic. During the exploration of the different values of P_{inf} , it has been found that the behaviour of the model is consistent with the description provided by the Population-based epidemiological models. A minimum threshold for the value of the parameter P_{inf} discriminates between the infections that extinguish and those that affect the whole system. In this sense, this minimum threshold is analogous to the reproduction factor (R_0) employed in continuous models. More specifically, P_{inf} plays the same role as the infection rate (β) in the SIR model, therefore $R_0 \propto P_{inf}$ (see Section 1.4.3).

Source of RBCs

Several studies indicate that *P. falciparum* has preference for infecting young RBCs. Firstly, age fractionation of RBC populations prior to cultivations shows that the growth ratios of the infection is significantly greater for those cultures performed with samples containing more reticulocytes (young RBCs aged < 7 days) (Pasvol et al., 1980). Secondly, studies of multiple infections confirm that the susceptibility to invasion of reticulocytes is 4-fold the susceptibility of older RBCs (Simpson et al., 1999).

Human RBCs for malaria cultures are usually obtained from outdated blood that is considered not usable for blood transfusions. This blood can be kept frozen (at temperatures that may reach -80°C) for several years without loss of harvest viability. Cultures with blood frozen for 19 months and 24 months do not show significant differences when compared with control cultures with fresh blood (Pavanand et al., 1974).

In addition, whatever is the source and keeping of RBCs, they must be prepared prior to the cultivation. They are washed and mixed with culture medium and usually subsequently stored at temperatures that range from 1°C to 1°C , prior to the cultivation. The time spent in these conditions affects the cultures performance. The blood storage regimes have influence on the RBC suitability when storage exceeds 3 or 4 weeks (Capps and Jensen, 1983). Cells can be used for up to 5 weeks of storage at 4°C and are typically maintained for 4 days to a week once washed (Trager, 1994).

To sum up, storage spans greater than the age of reticulocytes have no significant effect on RBC susceptibility to infection, but the performance of the infection still depends on this storage. Besides, significant differences on the parasite proliferation are observed

between cultures of young and old RBCs.

The hypothesis assumed in the model are: i) the parasite has a preference for young cells, and also detects their freshness, and; ii) storage ages RBCs reducing their freshness but without changing them. Presumably, low temperatures prevent the reticulocytes from turning into mature RBC forms. These assumptions are introduced in the model of the temporal evolution of P_{inf} in two ways:

1. as the abrupt decay on P_{inf} after a period in culture t_c that stands for the differences in the infection susceptibility observed for reticulocytes and older RBCs. This decay is introduced as an exponential factor modulating P_{inf} , with both the offset value and time constant equal to the 7-10 days (maximum age of reticulocytes). See Equation 2.4. Note: $t_c = t_{RBC} - t_{RBC}^*$, where t_{RBC}^* is the age at subcultivation; t_c does not include the storage time.
2. as a linear decay of the infection susceptibility with the RBC age (t_{RBC} , including storage time), from a maximum value P_{max} at age 0, until reaching a minimum value P_{min} at $t_{RBC} = t_{MRBC} = 120 \text{ days}$ (Guyton, 1987), which stands for the decrease in freshness of the RBC. See Equation 2.4. As mentioned above, variations on P_{max} , P_{min} and t_{MRBC} entail very small differences in the overall GR of the system.

A trial of virtual experiments to test this model consists on launching simulations similar to the *candle-jar* cultivation of the parasite where the subcultures are fed with RBCs that proceed from sources stored for different time spans. Two series of static cultures are simulated, with subcultivations that set the parasitaemia at the new culture to 0.5%, each 48 h and each 96 h, respectively. Initial parasitaemia is set to $\%I_0 = 0.5\%$ and infection probability to $P_{max} = 0.85$, $P_{min} = 0$, respectively.

Each trial explores culturing protocols where the subcultivation are carried out using increasingly old RBCs (Storage spans are set to: 0 days, 4 days, 8 days, 12 days, up to 3 months). The average parasitaemia of long-term cultures maintained for up to 3 months is compared for the different renovation protocols. The obtained results are presented in Figure 2.8.

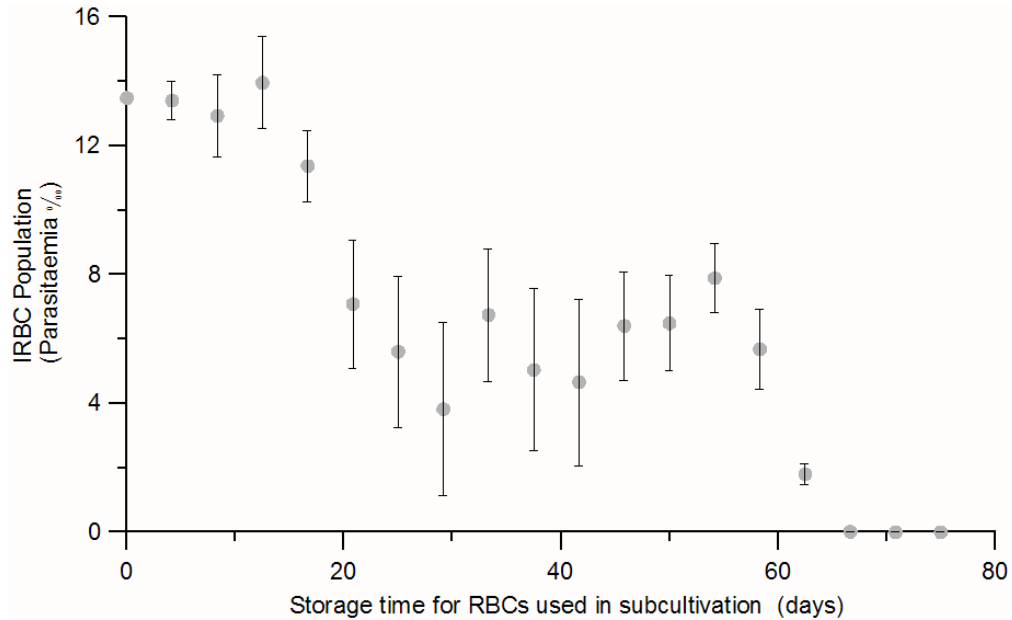


Figure 2.8: Simulations showing the modelled effect of the storage of RBCs on the culture performance. Average parasitaemia through the culture decreases with the storage time for the source of RBCs. Grey dots show the mean values obtained from two sets of simulation trials that performed subcultivations each 48 h and 96 h. Errors bars reflect the variability in the simulations.

These results show that under storage times < 16 days, the parasite can grow unhindered. After 20 days of RBC storage, the parasite can be maintained in culture with a parasitaemia slightly greater than the inoculum (indicating that there is no effective propagation of the infection, i.e. $GR \sim 1$). If the storage time is greater than 60 days, the viability of cultures is strongly limited.

The rules above presented allow reproducing the temporal evolutions observed in several cultures and provide an explanation for the reduced performance of the cultures where RBCs have been stored for long time, consistent with the experimental observations.

No virtual experiments on the multiple infection have been carried out with this version of the model because a rule limits the maximum number of multiple invasions on a RBC to 3 merozoites per RBC. This rule was introduced in response to the local limitations caused by the spatial structure of the model: up to 32 merozoites can be released from a IRBC at the end of the infection cycle, but each IRBC has 8 healthy RBC neighbours at most. Not introducing a maximum threshold for the number of multiple invasions led

to IRBCs infected with 5 or even 7 multiple invasions, which have never been observed in real systems.

Merozoite egress from IRBCs

At the end of each infection cycle merozoites are released to the extracellular medium ready to invade RBCs. The three alternative mechanisms for merozoite egress described in Section 1.2.2, are represented by three mutually exclusive rules (see Figure 2.9):

(i) Membrane fusion: all the merozoites are released into a single spatial cell, chosen from one of the nearest neighbours of the IRBC ($\sim 10 \mu m$).

(ii) Membrane breakdown: each of the merozoites has a probability of being released into one of the nearest neighbour spatial cells including the same cell ($\sim 10 \mu m$).

(iii) Exploding flowers: egressing merozoites are randomly distributed among the neighbour spatial cells up to a range of 2-3 spatial cells distance ($\sim 25 \mu m$). The probability of being dumped into a particular spatial cell linearly decreases with the distance to the source IRBC. The set of probabilities is normalized.

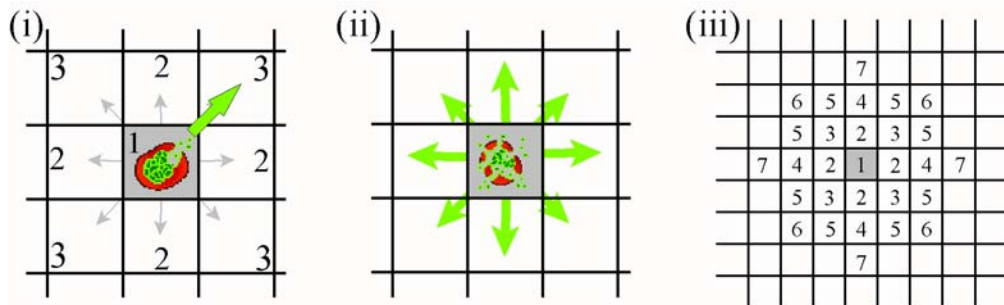


Figure 2.9: Stencils of the models of merozoite egress from IRBCs at the end of the infection cycle (lysis occurring at the grey central spatial cell). i) Membrane fusion: all merozoites are released to one of the nearest neighbour cells with a probability $P(1)=0.4$, $P(2)=0.1$ and $P(3)=0.05$; ii) Membrane breakdown: merozoites are scattered around, each merozoite is dumped into one of the nearest neighbor cells with the same probabilities as (i); iii) Exploding flowers: Long range egress. The probabilities of a merozoite being dumped into each cell are: $P(1)=0.212$, $P(2)=0.053$, $P(3)=0.037$, $P(4)=0.026$, $P(5)=0.022$, $P(6)=0.019$ and $P(7)=0.018$.

Each mechanism of merozoite egress has been introduced into the model. The outcome of the 8-days simulation of a closed system has been carried out assuming that the values for all the parameters are fixed and similar to the ones used in the simulation of the *candle-jar* experiments ($\%I_0 = 0.1\%$, semisynchronous inocula, $P_{max} = 0.8$ and $DP(S) = 0.005$,

$DP(F) = 0.01$).

In addition, the effect of the spatial structure on the infection process has been assessed for each mechanism. The scale of the spatial cell side has been modified to allow up to 1, 2 3 or 4 RBCs per spatial cell. 10 different simulations of 8-day static cultures have been carried out for cultures with different RBC densities and no accidental death rate ($DP = 0$). The obtained results show:

- i) The puntual egress of merozoites leads to infections that do not propagate through the hematocrite, $GR_{24} \leq 1$. Unless $DP = 0$, the parasitaemia fades out until there are no IRBCs, $GR_{24} < 1$. Increasing the RBC density ($\rho_{RBC} = \frac{N^{\circ} RBCs}{spatial\ cell}$) leads to an increase in the parasitaemia and in the infection daily growth ratio, $GR_{24} > 1$. The maximum observed growth ratios are achieved with 4 RBCs/spatial cell: $GR_{24} = 1.8$ (between day 7 and day 8 in Figure 2.9.a) and $GR_{48} = 2.3$ (between day 6 and day 8 in Figure 2.10.a), respectively. The growth ratio per infection cycle increases with cell density and rapidly gets saturated around $GR_{48} = 2.5$ (see Figure 2.10.b).
- ii) The egress of merozoites at one of the nearses neighbour spatial cells reproduces the infection propagation rates. Average simulation growth ratios range from $GR_{48} = 4.5$, when there is 1 RBC per spatial cell (which is consistent with the behaviour observed in real cultures), to $GR_{48} = 10$ for 10 RBCs/sc. The effect of the spatial structure on the parasite proliferation is depicted in Figure 2.10.b. The growth ratio increases with the number of RBCs/sc but gets saturated around $GR_{48} = 12$. This is consistent with the expected behaviour in real systems if there were no limitations due to the local spreading of merozoites or the availability orf RBCs, since ~ 16 merozoites on average are released in the lysis at the end of each infection cycle and the probability of invading a healthy RBC is (at the most) smaller than one.
- iii) When merozoites are released to a fairly extensive area around the IRBC (for instance, the two first layers of first neighbour cells) the simulation outcome shows growth ratios that reach values far greater than those observed in real systems $GR_{24} = 14$ and $GR_{48} = 25$. The average value obtained with the 10 simulations with 1RBC/sc is $\langle GR_{48} \rangle = 15$. This parasite multiplication ratio already exceeds the behaviour observed in real cultures, so no further simulations increasing the number of RBC per spatial cell have been carried out.

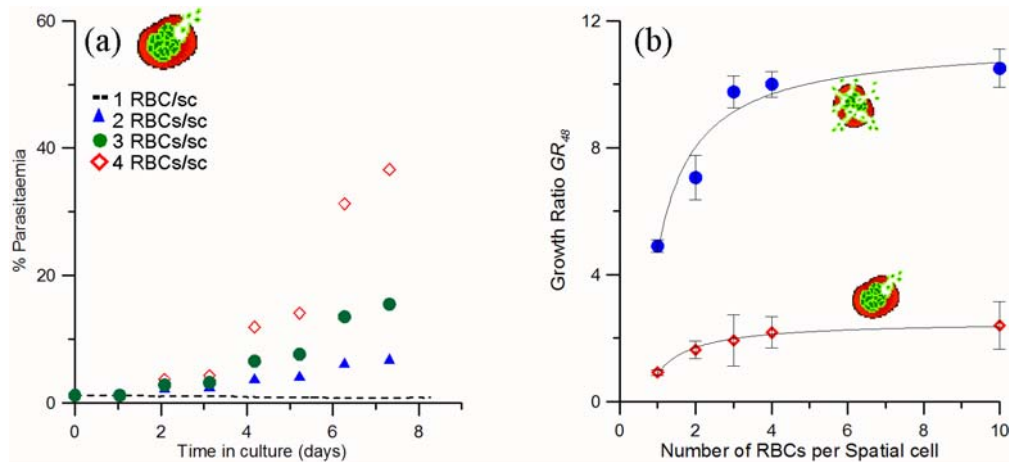


Figure 2.10: *Simulation results of the different models for merozoite egress. a) Temporal evolution of the parasitaemia for different cell densities according to the membrane fusion model (punctual egress of merozoites). Dashed line (-) represents 1RBC per spatial cell (RBC/sc); Triangles (\blacktriangle) represent 2RBC/sc; Solid dots (\bullet) represent 3 RBC/sc; Diamonds (\blacklozenge) represent 4RBC/sc. b) Comparison between the growth ratios predicted for different cell densities by two different egress models: dots (\bullet) stand for the membrane breakdown model (scattered merozoites) and diamonds (\blacklozenge) stand for membrane fusion model. The former agrees better with experimental results.*

The results provided by the model suggest that the membrane breakdown is the mechanism through which merozoites egress from IRBCs at the end of an infection cycle. These results are consistent with recent experimental observations (Rayner., 2006).

Serum and culture medium

The cultivation of *P. falciparum* requires the use of human serum to provide the proteins and aminoacids to the parasite inside the IRBC. As it is an scarce resource, proposals for alternative serum sources (natural and sythetized) can be found in literature (Jensen, 1988; Trager, 1994). Today, several companies provide commercial serums with different specifications.

In order to assess the appropriateness of different commercial culture mediums, the group EMG-GSK performed a series of experiments consisting on 1-week cultivation of the same strain of *P. falciparum* with same blood source under the experimental conditions detailed in Table 1.2 and with different culture medium and degree of synchronism of the inoculum. Initial parasitaemia was set to $\%I_0 \sim 1\%$ and the degree of synchronism

was qualitatively assessed only distinguishing between synchronous and asynchronous inocula. The experimental results are outlined in Table 2.7. A more detailed description is presented in Appendix B (B.1).

Days in culture	Medium A				Medium B		Medium C			
	S.		A.		S.		A.		S.	
	% I_{obs}	% I_{calc}	% I_{obs}	% I_{calc}	% I_{obs}	% I_{calc}	% I_{obs}	% I_{calc}	% I_{obs}	% I_{calc}
0	1	1	1	1	1	1	0.95	0.95	1	1
1	1.3	1.3	3.3	3.3	1.3	2.8	2.3	2.3	1.9	1.9
2	7.8	7.8	3.4 _($\frac{1}{4}$)	13.6	4.4	4.4	5.7	5.7	1.9	1.9
3	7.6	7.6	-	-	4.8	4.8	3 _($\frac{1}{4}$)	12	3.8 _($\frac{1}{4}$)	11.5
4	4 _($\frac{1}{4}$)	16	2.9 _($\frac{1}{4}$)	47.7	2.9 _($\frac{1}{4}$)	11.4	7.7	30.8	11.6	32.8
5	-	-	3.8	60.3	-	-	-	-	-	-
6	-	-	-	-	-	-	-	-	-	-
7	10.2	40.8	-	-	7.9	31.8	-	-	-	-
$GR \pm \sigma$	3 ± 2		3.0 ± 1.2		2.5 ± 0.9		2.9 ± 0.7		2.7 ± 1.4	

Table 2.7: Cultivation of *P. falciparum* using 3 different commercial culture mediums. S.: Synchronous inoculum; A.: Asynchronous inoculum; observed (% I_{obs}) and calculated (% I_{calc}) parasitaemias; GR: average observed growth rate and deviation (σ_{GR}). The subscript fraction in brackets in the observations column indicates the dilution carried out during the subcultivation prior to measurement, i.e. the fraction of replaced RBCs; - indicates no experimental measurements. Experiments performed the EMG-GSK.

The statistical analysis of the calculated parasitaemias % I_{calc} with ANOVA (or the simpler comparison of daily growth ratios GR_{24}) shows: i) that the choice of one of these culture mediums does not significantly affect the propagation of the infection; ii) that synchronous and asynchronous inocula behave in a similar way, both when comparing the behaviour for each culture medium separately and when considering the subsets of synchronous and asynchronous trials.

INDISIM-RBC does not include information regarding the exhaustive composition of the extracellular medium, nor a detailed description RBC's metabolism. The effect of the different culture mediums is introduced into the model as variations in the values of the accidental death probability (P_{death}). Post-invasion time distributions among the inoculated IRBCs are considered uniform, with an amplitude $t_{INF}^{MAX}(t=0)$ that decreases with the observed degree of synchronism. The initial values of % I_0 are set according to the input measured values (at day 0), infection probability is set to $P_{max} = 0.85$, $P_{min} = 0$, and P_{death} is modified from culture medium to culture medium. A reproduction of three sample cultures is depicted in Figure 2.11.

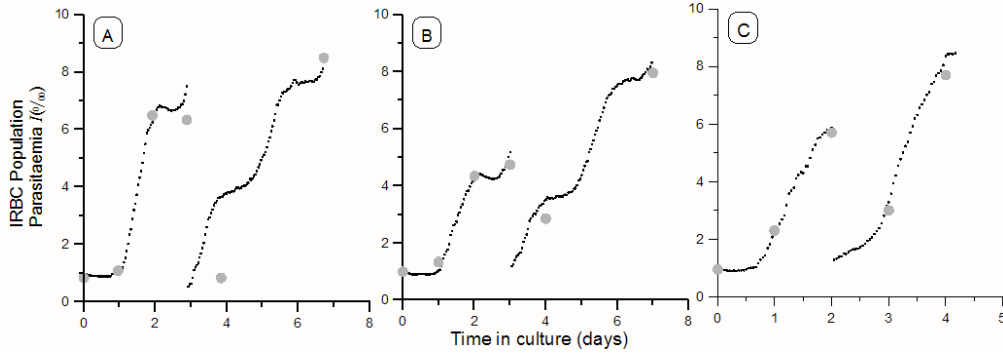


Figure 2.11: *Experimental results compared to simulation outcome for cultures using different culturing mediums. Grey dots correspond to a 7 day trial measurement. Black small dots correspond to simulation outcome. a) Culture medium A (S.), synchronous inoculum with 100% Rings; $P_{death}(T) = 0.001$, $P_{death}(S) = 0.007$, $P_{death}(F) = 0.01$ and $t_{INF}^{MAX}(t = 0) = 20$ ts; b) Culture medium B (S.), synchronous inoculum with 90% Rings; $P_{death}(T) = 0.001$, $P_{death}(S) = 0.01$, $P_{death}(F) = 0.01$ and $t_{INF}^{MAX}(t = 0) = 25$ ts; c) Culture medium C (A.), asynchronous inoculum with $< 80\%$ Rings; $P_{death}(T) = 0.001$, $P_{death}(S) = 0.005$, $P_{death}(F) = 0.02$ and $t_{INF}^{MAX}(t = 0) = 35$ ts.*

2.3.4 Synchronizaton of the infection process

The degree of synchronism of the inoculated IRBCs has little effect on the long-term cultivation of *P. falciparum* because, typically, *in vitro* synchronisation of the parasite population disappears during the infection course (Kiatkowski, 1989). The statistical analysis of the simulation results that represent the short-term cultures in Table 2.7 show similar conclusions to those drawn from the analysis of experimental data: no significant differences can be found in the culture performance (GR) between cultures with synchronous and asynchronous inocula. Nevertheless, simulations show different behaviours depending on the degree of synchronism of the inoculum ($t_{INF}^{MAX}(t = 0)$). For instance, the lag period until the disease spreads through the hematocrite (τ_{lag}) is $\tau_{lag} = 48 - t_{INF}^{MAX}$.

On the other hand, *P. falciparum* schizogony is stably synchronized for long-term *in vitro* cultures only when specific manipulations are carried out, e.g.: sudden increase in temperature or treatment with sorbitol, among others (MR4, 2008; Kiatkowski, 1989). These treatments mostly affect IRBCs in mature stages of the infection cycle and leave young ring-stages (post-invasion times $t_{INF} < \sim 15$ ts) unharmed. Particularly, the procedure to synchronize parasites with sorbitol requires repeating the treatment twice in 48h to guarantee that only ring forms are left. To keep the parasites synchronized, the sorbitol treatment must be performed once a week.

Modeled IRBC populations naturally become desynchronized as a consequence of the variability in the duration of the infection cycles (see Figure 2.12). Synchronous IRBC populations can be obtained through the punctual removal of the mature part of the IRBC population to represent specific synchronizing treatments. In this case, a rule introduced *ad hoc* forces the system as a whole to synchronize.

Noteworthy, stage-dependent death probabilities $P_{death}(0, R, T, S \text{ and } F)$, together with periodic subcultivation also limit the degree of desynchronization of IRBC population (see Figures 2.12 and 2.13). In this case, the preservation of certain synchronism emerges from rules that do not directly impose the coordination of the population.

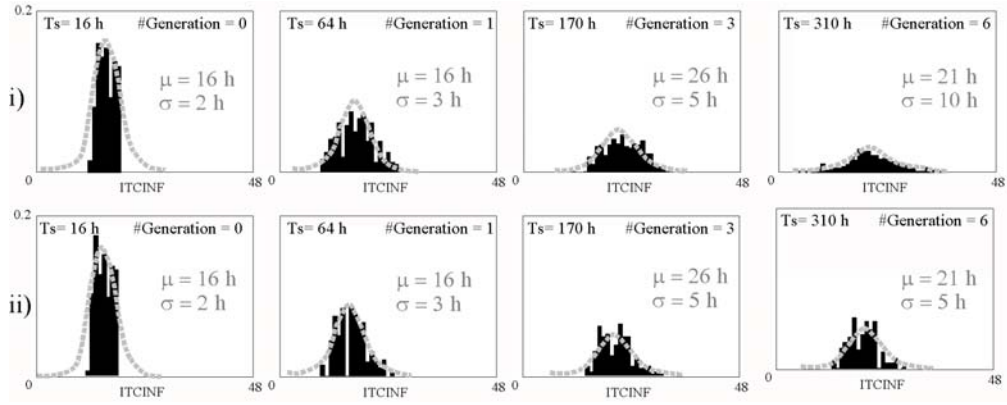


Figure 2.12: *Simulated post-invasion-time distributions among the IRBCs (outcome from model 2Dv.2). Relative frequency vs. post invasion time (t_{INF}). T_s indicates the time in culture of the sample, #Generation stands for the number of completed infection cycles in the culture. Synchronous homogeneous inoculum: $t_{INF}^{MAX}(t=0) = 20 t_s$, 2 hours. Variability in the duration of the infection cycle: $\sigma = 2$ hr. i) IRBC population gets desynchronised in cultures with $DP(\nabla) = 0$ and no subcultivation; ii) synchronism is maintained by the staggered death of IRBCs ($P_{death}(F) = 0.001$) and periodic 96 hr subcultivation. Grey dashed lines show the best-fitting normal distributions, with mean value μ and standard deviation σ .*

Appart from synchronising the IRBC population, the use of a staggered P_{death} applied at each time step entails the reduction of the viability of the infection. The number of IRBCs in INDISIM is analogous to $I(t)$ in the SIR model, and increasing P_{death} is analogous to an increase in the recovery/mortality rate γ (see Equation 1.2 in Section 1.4.3). This can be derived from the individual scope: the reproduction factor of the infection (R_0) is proportional to the number of IRBC that successfully undergo a complete infection cycle ($P_{survival}$).

$$R_0 \propto P_{inf} \cdot P_{survival} \quad (2.7)$$

The probability of survival for IRBCs undergoing a complete infection cycle is the joint probability of the IRBC surviving each time step $p_{survival}(ts)$, all through the infection cycle $t_{INF} = [1, t_{MINF}]$.

$$P_{survival} = \prod_{t_{INF}=1}^{t_{MINF}} p_{survival}(t_{INF}) \quad (2.8)$$

In turn, surviving is the complementary event of dying. Then,

$$p_{survival}(ts) = 1 - P_{death}(ts) \quad (2.9)$$

Combining 2.8 and 2.9, we find:

$$P_{survival} = \prod_{t_{INF}=1}^{t_{MINF}} [1 - P_{death}(t_{INF})] = P_{death}(R)^{t_{MCL}(R)} \cdot P_{death}(T)^{t_{MCL}(T)} \cdot P_{death}(S)^{t_{MCL}(S)} \cdot P_{death}(F)^{t_{MCL}(F)} \quad (2.10)$$

The custom values of DP in version *2Dv.1*, *2Dv.2* and *v3D* (see Table 2.1) entail the effective survival of the IRBCs $P_{survival} = 0.9$. Particularly, the probabilities obtained using the values used to simulate the short-term preservation (see Table 2.3 in Section 2.3.1) and the long-term cultivation (see Table 2.4 Section 2.3.2) of the parasite are: $P_{survival}(short - term) = 0.6$ and $P_{survival}(long - term) = 0.9$, respectively.

A simple mathematical model describing the population structure in *P. falciparum* IRBCs was developed to understand infection dynamics *in vivo* (White *et al.*, 1992). The White-Chapman-Watt model (WCW) considers that IRBC post-invasion times are normally distributed and uses two parameters only; the mean (μ) and the standard deviation (σ_μ). At any time (ts), the post-invasion time distribution is represented with the function $q(t_{INF})$. If the infection is fairly synchronous ($\sigma < 12 h$), this function is composed by the underlying intrinsic distribution of parasite stages of the current generation (a normal distribution $f_{ts}(t_{INF})$) and the contribution of the previous generation ($p_{ts}(t_{INF})$ represents the left tail of the last infection cycle) and next generation of parasites ($n_{ts}(t_{INF})$ represents the right tail of the next infection cycle). Such shape is no longer observable if the infection cycle is highly asynchronous (see Figure 2.13a). The WCW model predicts a log linear rise in the parasitaemia for asynchronous cultures that becomes increasingly terraced with the degree of synchronism of the IRBC population (see Figure 2.13b).

Long-term cultivation of synchronous IRBC populations with periodic subcultivations at 96 hours has been compared to the WCW predictions on the parasitaemia-time curves

of an unimodal IRBC population. The observed left-handed bents on the peaks of the parasitaemia are consistent with the skew to younger IRBC forms induced by a staggered P_{death} (see Figure 2.13c). The simulations are carried out using the version *2Dv.2* operating at conditions similar to the *candle-jar* protocols, with fixed death probabilities $P_{death}(S) = 0.002$ and $P_{death}(F) = 0.005$. These values for P_{death} result in a probability of completing the infection cycle per IRBC equal to $P_{survival} = 0.64$.

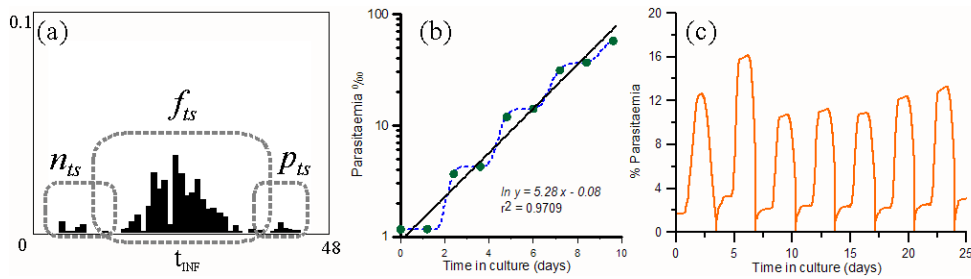


Figure 2.13: *Outcome of the Individual-based model compared to the predictions of a continuous model (White et al., 1992); a) The post-invasion time distribution is composed by the intrinsic distribution of the IRBCs of an infection generation (f_{ts}) plus the contributions of past (p_{ts}) and next (n_{ts}) generations; b) log linear rise of parasitaemia in an unlimited culture. Simulation outcome at each time step (dashed line) and daily samples (\bullet). Terraces and steeps smooth in successive infection cycles. Corresponding asynchronous evolution (solid line). Corresponding daily growth ratio, $GR_{24} = 5.28$, is compatible with the values typically observed in real systems; c) Long-term cultivation of a synchronous culture with a 4-day subculturing period.*

2.3.5 Substrate availability

Standard glucose and lactate concentrations in the RBC culture medium are $[gluc.] = 2.6 \text{ mM}$ and $[lact.] = 0 \text{ mM}$, respectively. Maximum rates of metabolized glucose and lactate produced are: $\frac{d[gluc.]}{dt} = \frac{-(122 \pm 34) \mu\text{M}}{10^9 \text{ RBCs} \cdot \text{day}}$ and $\frac{d[lact.]}{dt} = \frac{(143 \pm 47) \mu\text{M}}{10^9 \text{ RBCs} \cdot \text{day}}$. Finally, adequate *in vitro* parasitaemia yields are obtained when $[lact.] = 12 \text{ mM}$ (Jensen et al., 1983). Considering this data together, global limitations on the parasite development caused by the scarcity of glucose or the excess of lactate are expected not before 20 days.

Nevertheless, heuristic knowledge on the handling of *in vitro* cultures suggest that the culture medium should be replaced every two or three days at most, and it is commonly accepted that this requisite is brought by the substrate limitations on the parasite. Moreover, it has been claimed that unrestricted parasitaemia yields can be obtained by

increasing the fraction volume of medium per volume of the hematocrit, which indicates that the concentration of substrate is somehow determinant for parasite viability (MR4, 2008). Specific trial cultivations carried out by the EMG-GSK show that, under standard static culturing conditions, closed systems can be maintained up to 72 hours, at most (see Appendix B, B.2).

Trials with continuous cultures assuming different regimes for the medium renewal show that no significant differences are found between cultures with periodic subcultivations each 48 h and each 72 h (see Appendix B, B.3). Figure 2.14 shows the time course of both kind of actuation patterns in two replicas of 10-day cultures. Replicate cultures show identical evolutions. Similar values for the maximum parasitemia ($\%I_{max}$) and the growth ratio are obtained in both subcultivation protocols: $\%I_{max} = 4.9\%$ and $GR_{24} = 2.7 \pm 1.0$ for the 48 h actuation pattern; and $\%I_{max} = 4.6\%$ and $GR_{24} = 2.2 \pm 0.9$ for the 72 h actuation pattern.

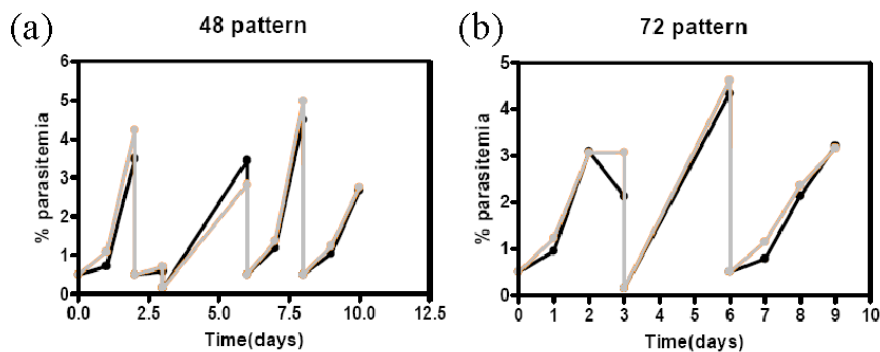


Figure 2.14: Temporal evolution of the parasitaemia for different subcultivation protocols. a) Periodic subcultures performed each 48 h, and b) periodic subcultures performed each 72 h. Grey and black solid lines and dots correspond to the two replica of experimental data.

The nutrient limitations in closed *in vitro* cultures have been studied through the exploration of the outcome of INDISIM-RBC, which considers glycolysis as the only metabolism for RBCs and IRBCs. Results show that in culturing conditions glucose is the limiting factor, rather than lactate. Simulations of closed systems recreating the current culturing medium to hematocrit ratios suggest that generalised scarcity of glucose resulting in massive death of IRBCs does not take place (see Figure 2.15a). Threshold parasitaemia yields appear after more than 10 days in culture and at parasitaemias around $\%I = 60\%$. Increasing 100-fold glucose concentration allows reaching $\%I = 100\%$

parasitaemias, and massive extinction occurs after more than 10 days, in this case as a consequence of excessive lactate. The massive death of RBCs when these threshold values are achieved does not entail the decrease of the observed parasitaemia.

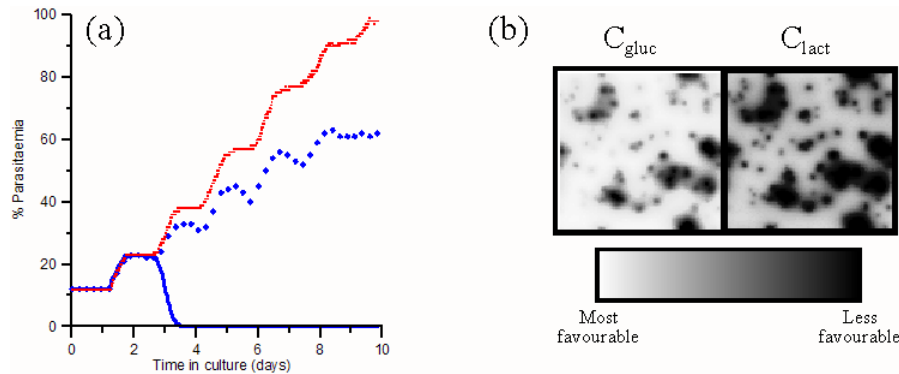


Figure 2.15: *Simulated nutrient limitations on the propagation of the infection; a) Parasitaemia evolution in closed culture systems for different overall initial concentrations of glucose; diamonds (\blacklozenge) represent $C_{gluc}(t=0) = 2.6 \mu M$, dotted line (\cdots) $C_{gluc}(t=0) = 0.26 \mu M$ and solid line ($-$) $C_{gluc}(t=0) = 0.026 \mu M$; b) Autoscaled visualisation of local concentration of glucose and lactate show that glucose is a more limiting factor to the parasite proliferation.*

The results obtained with INDISIM-RBC do not reproduce the observations of real systems. The decay of the infection after three days that is observed in real cultures only appears in the simulations when considering glucose concentrations around 100 times smaller than those of real cultures. These results suggest that the model of the individual metabolism leaves a key factor that limits the proliferation of the parasite. Despite this shortcoming, results shown in Figure 2.15a can be positively used: INDISIM-RBC is consistent with overall limitations appearing after three days in culture, caused by scarcity of some other limiting compound. Remarkably, these limitations appear when the parasitaemia is around $\%I \sim 20\%$. This is also consistent with the experimental observations.

Limitations at a local level appear when the overall conditions are not favourable enough. INDISIM-RBC shows that conditions nearby the foci of the infection are less favourable to RBC viability. Figure 2.15b shows that around the IRBCs glucose is scarce and lactate accumulates. RBCs are more susceptible of not being able to fulfill their metabolic needs near an infected region. The advantage of focusing on local limitations is that they can be skipped with simple manipulations of the culture that modify the spatial structure of the hematocrit (see Section 2.3.6).

INDISIM-RBC-2*Dv*.2 was designed to better account for the factors at a local scale that might be responsible for the limitations observed in real systems. In this version, the temporal scale is reduced with the aim of better capturing the diffusion of substrate and the spreading of the parasite. The results obtained with the improved version still do not show local limitations on the IRBC viability with the real glucose and lactate concentrations. Again, this suggest that either i) there is another metabolic limiting factor, ii) the algorithm used to represent the diffusion of substances through the hematocrit at the current scales is still insufficient, or iii) the current two dimensional approach cover the phenomenon occurring in the real hematocrit layer. The diffusion problem in 3D is revisited in Section 3.5.

2.3.6 Agitation of the culture systems

An alternative to the static cultivation of *P. falciparum* (where the RBCs remain settled forming a hematocrit layer at the bottom of culture vials) is the cultivation in suspension (where a slurry formed by RBCs and medium is maintained through the continual agitation of the culture system). Suspended cultures have been claimed to render more abundant harvests than static cultures (Butcher, 1981). Apparently, they show increased infection growth ratios (Butcher, 1982) and support higher parasite yields (Zolg et al., 1982) without unaffordable medium expenses. Furthermore, a method using low hematocrit and high glucose content apparently only required to be sucultured each 3 days without medium replacement in between (Fairlamb et al., 1985). These published experimental results do not provide strictly conclusive evidences to support the preference of IRBCs for suspended cultures, although they clearly point in this direction.

The expected behaviour of the suspension systems is the compromise between two opposite trends:

1. on the one hand, the continual shift of positions of the RBCs favours the propagation of the disease because the number of potential healthy RBC targets to be invaded by an egressed merozoite is no longer restricted to the immediate neighbourhood of the lysing IRBC. In addition, the mix of the hematocrit layer homogenizes the concentration of solute substances, therefore vanishing the effect of local substrate limitations.
2. on the other hand, the reduction of cell density hinders the propagation of the infection in suspended cultures. This can be understood as the decrease in the probability of encounter between a merozoite and IRBC due to a reduced density, which consequently reduces the rate of transmission.

In addition, the death probability is likely to be increased when the RBCs are submitted to the damaging methods usually employed to maintain cells in suspension (i.e. airlift columns or stirring, shaking or wagging of the culture systems). Moreover, the continual movement of RBCs could hinder the attachment and invasion of healthy RBCs by merozoites, reducing the infection rate.

Discrete agitation regimes

The arguments above suggest that the agitation of static culture systems at discrete time spans would increase the performance of static *in vitro* cultivation of *P. falciparum*. Indeed, discrete gentle agitation of the hematocrit combines the increase in the number of potential healthy RBC targets (trend 1) with the high cell densities within the hematocrit layer (trend 2). In addition, the potentially harmful effects of agitation are reduced.

Data in literature suggest that typical RBC sedimentation rates are around $v_{sed}(RBC) = (2.10 \pm 0.18) \cdot 10^{-3} cm/s$ (Neu and Meiselman, 2001). Settling of RBCs after agitation would take between two or three minutes for custom culture systems with $H_{culture} \sim 2 mm$ height (MR4, 2008). Measurements of the RBC sedimentation rate carried out by the EMG-GSK in cultures with several heights provided significantly different results, $v_{sed}(RBC) = (1.1 \pm 0.3) \cdot 10^{-5} cm/s$, which entail settling times of the order of $\sim 1 h$ (see Appendix B B.6). Nevertheless, culture systems submitted to gentle punctual agitations at big enough regular spans ($T_{agitation} > 12 h$) can be regarded as static cultures, because this assumption holds for more than 90% of the time in culture.

Discretely agitated static cultures have been implemented by the EMG-GSK. The comparison of the short-term cultivation of the parasite in closed systems under different discrete agitation regimes shows no significant differences between the cultures agitated each 24 h, 48 h and 72 h (see Appendix B B.2). Closed cultures last for three days at most (no viable forms are observed in the sample at 96 h), show maximum parasitaemias around $\%I \sim 5\%$ and growth ratios in the range $6 < GR_{48} < 10$. No correlation can be observed between the agitation regime and the growth ratio. For this reason, no experiments of the long term cultivation of discretely agitated cultures have been carried out.

Discretely agitated culture systems are represented by INDISIM-RBC as static cultures where the positions of RBCs are periodically shifted at each agitation. INDISIM-RBC shows no differences between the behaviour static cultures and discretely agitated cultures with different agitation periods. The results obtained in real and simulated cultures suggest that either the local limitations (regarding the spreading of the parasite and/or the concentration of substances in solution) are not overcome with discrete agitation, or that there are no such local limitations.

Cultivation of *P. falciparum* in suspended cultures

The EMG-GSK has performed several trial experiments to assess the differences between static and suspension culture systems. Suspension cultures are carried out through the continuous agitation of the system with a magnetic stirrer operating at non-damaging velocities (see Appendix B B.2). Trials in closed culture systems show that stirred cultures grow at significantly higher rates than static or discretely agitated cultures do. Nevertheless, like the other closed systems, suspension cultures are still submitted to overall limitations that do not allow the viability of IRBCs after 72 *h*. These results suggest that limitations on the spreading of the infection, exist both at a local and at a global level.

The positive results of cultures in suspension bring about the trial of long term continuous cultivation under different agitation regimes (see Appendix B B.4). The growth ratios observed in the continuous trials, $GR_{24}(stirred) = 3.7 \pm 1.7$ and $GR_{24}(static) = 1.8 \pm 0.6$, can be used to build a simple population-based model for the spreading of the infection between two successive subcultivations. This model assumes unrestricted propagation of the parasite and fits an exponential function to the observed growth ratios. The parasitaemia at each time step after subculturing are obtained with:

$$\%I_{stirred}(ts) = 0.5\% \cdot e^{0.05/hr \cdot ts} \quad (2.11)$$

and

$$\%I_{static}(ts) = 0.5\% \cdot e^{0.023/hr \cdot ts} \quad (2.12)$$

As discussed in Section 2.3.5, these models are only valid for low parasitaemias and provide unrealistic parasitaemias after 3 days in culture, because unrestricted proliferation of the infection can not be assumed indefinitely. Still, the models represented by 2.12 and 2.11 can be considered valid enough during the first 72 *h* and can be used to predict the behaviour of different subcultivation regimes for static and stirred cultures maintained for a month. Two different subculturing protocols are trialed with the purpose of using an automated culturing device. Both consist on performing periodic subcultivations each 48 *h*, but the dilution fraction of culture RBCs to freshly added RBCs is performed differently. The traditional man-made renovation sets parasitaemia to 0.5% after subculture, while the semiautomated renovation carries out a constant RBC dilution that leads to the same parasitaemia, according to the growth rate predicted by the continuous model (see Equations 2.11 and 2.12). Dilutions in semiautomated subculturing are set to $f_{stirred} = \frac{1}{11}$ and $f_{static} = \frac{1}{3}$, respectively. The experimental results are shown in Figure

2.16. The predictions of the continuous model are not significantly different from the experimental observations.

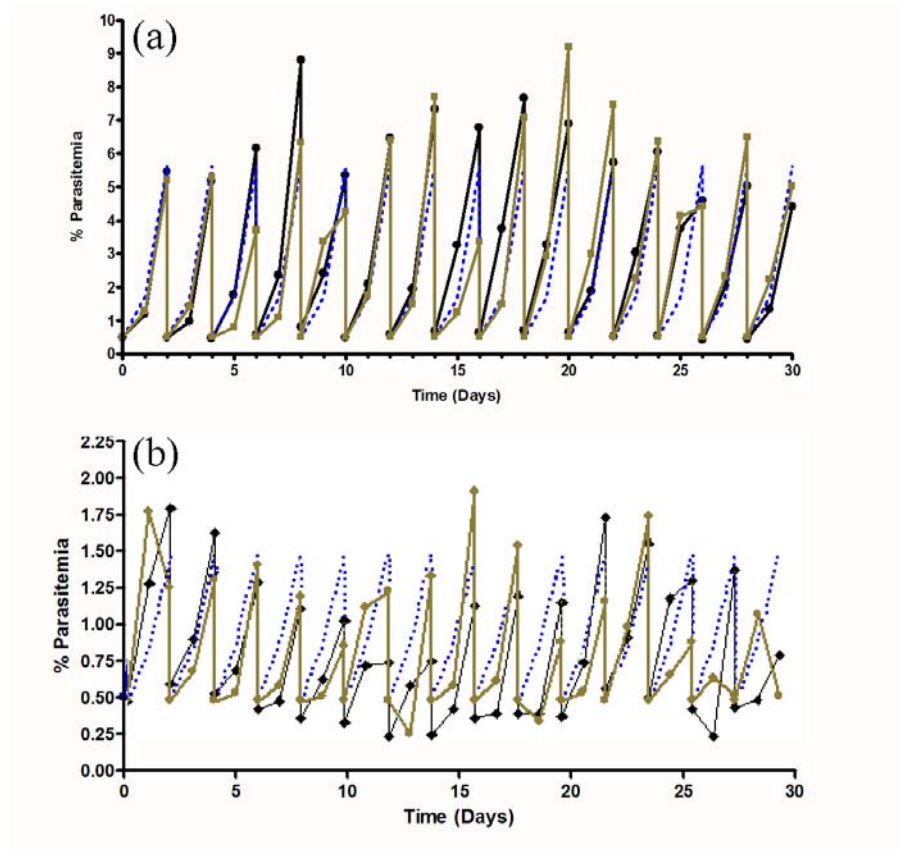


Figure 2.16: Course of the parasitaemia, observed daily in stirred (a) and static (b) long-term cultivation of *P. falciparum* infected RBCs (see Appendix B B.5) and compared to the predictions by equations 2.11 and 2.12, respectively. Green solid line corresponds to a culture with daily human subcultivation, to set the initial parasitaemia $\%I_0 = 0.5$ after subculture. Blue dotted line shows the expected behaviour of automatized subcultivation with ratios $f(a) = \frac{1}{11}$ and $f(b) = \frac{1}{3}$ predicted by the model. Black solid line shows the measurements of real automatized cultures.

Suspension can be represented by INDISIM-RBC as a custom static model with two modifications:

1. The system is continuously mixed. At each time step, the position of the RBCs is shifted at random, merozoites are scattered all through the spatial cells and

substrate is continuously homogenized.

2. The RBC density corresponds to the volumetric hematocrit concentration (ranging from 5% to 10% in volume) rather than to the cell density observed in the hematocrit layer (where around 80% of the volume is occupied by RBCs). This marked reduction in cell density is introduced in the model as a decrease in the total number of modelled RBCs. For instance, in a model with 100×100 spatial cells, the representation of a static cultivation entails considering up to 10000 RBCs, while only 500 RBCs are included when modelling a suspended culture.

From the model outcome and the experimental results for the static and stirred cultures, one can state that both processes can not be reproduced simultaneously with the same set of individual-related parameters: simulation results show that the combination of mechanisms 1 and 2 using the values for P_{inf} and P_{death} that best fit static cultures lead to non-viable cultures. Moreover, finding a pair of values that reproduce the behaviours of real systems is quite difficult and the simulation outcomes show much more uncertainty than the observed for static cultures.

It is reasonable to assume that the values of the probability of infection and the damage caused to the cells is different in static and stirred cultures. Firstly, invasion of a healthy RBC by a merozoite placed at its same spatial cell when both cells are settled in the hematocrit gently touching each other is a process that clearly differs from the infection when both cells collide while drifting around. Secondly, cells submitted to any kind of agitation are necessarily exposed to more mechanical stress, and they can be damaged more easily. Several experiments carried out by EMG-GSK, which are not included in this work because they concern the development of a bioreactor, corroborate this assumption.

A more detailed study of agitated culture systems requires modifying the current versions of the model. Additional or alternative hypothesis regarding cell-cell interactions must be introduced into the model to tackle cultures in suspension.

2.4 Discussion and open questions

INDISIM-RBC proposes a set of rules governing individuals (RBCs and IRBCs) and their local environment (the spatial structure of the system, the extracellular parasite and substrate concentration in the culture medium) that can be used to better understand the behaviour of *Plasmodium falciparum* infected erythrocytes *in vitro* cultures. Several

patterns observed in real systems have been used to guide the design and development of the model:

1. *Population structure*: Post-invasion time distributions among IRBCs in short-term and long-term culture systems are quantitatively reproduced by the model.
2. *Population dynamics*: Temporal evolution of the observed parasitaemia and average infection growth rates at different time spans (24, 48, 72 and 96 hours) are quantitatively reproduced by the model.
3. *Population variability*: The trends and variability observed for cultures with different population structures regarding healthy RBCs (age distribution associated to different storage times) and infected RBCs (post-invasion time distribution) are also found in the model outcome.
4. *Infection structure*: several mechanisms of local spreading of the parasite and their resulting modelled infection dynamics are compared to experimental results. The model outcome that is most compatible with the real system-level observations corresponds with the mechanism that is most consistent with the behaviour of the parasite reported from individual imaging.
5. *Infection dynamics*: the relation between infection dynamics, IRBC population structure and culturing protocols is consistent with the observation of long-term culture system and with the predictions of accepted Population-based models.
6. *Infection variability*: The variability observed for experimental cultures of different strains of *P. falciparum* with different infection capability is also found in the model outcome.

This provides a due degree of confidence in the proposed mechanisms and in the underlying structure of the model. Taking the idea a bit further, it can be stated that the quantitative reproduction of a single sort of experimental results alone would not be an appropriate strategy to analyze and validate INDISIM. This can be argued as follows: experimental *in vitro* cultures of *P. falciparum* infected RBCs are complex systems that show both predictable features (patterns) and an erratic behaviours (variability). They are conditioned by coupled factors (strain of parasites, RBC source, culturing protocols...) that can not be disentangled one from each other, and which are hardly assessed through direct measurements. Even the simplest model that expects to capture the essential mechanisms that govern the culture evolution must be quite complex. INDISIM aims to be a tool to generate understanding of the system, thus explores these mechanisms by

putting together the theoretical insight regarding the RBCs and parasites. Therefore, it must assume several hypothesis at the same time, each of them concerning a particular aspect or process, and being represented by a set of equations and parameters. As a consequence, the model has too many degrees of freedom to be compared to a single variety of experimental results (a.k.a. pattern).

The systematic adjustment the model outcome to a single pattern for different experiments is an strategy to delimit the variability of the system under study and provides valuable insight. Indeed, the time course and average growth ratio of the parasitaemia for models of different experimental cultures have been widely used in this work as the reference to build the different parts of the model and as an acid test for its overall behaviour. Yet, this criterium alone does not provide enough arguments to hold the model. The degree of confidence in that the model is not a mere artifact increases when several independent patterns at different scales are reproduced. Two examples of independent patterns used here are the age distribution of RBCs and the post-invasion time distribution of IRBCs among the population, and their evolution all through the culture. The reproduction of different non-related patterns entails, at any rate, that even if the proposed mechanisms are just artifacts, they capture many aspects of reality. It also gives consistency to the model predictions regarding other patterns and increases its robustness: if any observation contradicts the model predictions, the required correction of the model should preferably preserve the reproduction of patterns that are already correctly simulated by the model.

Up to the moment, the model has been focused on the processes regarding the individuals and population structure, and on their relations with characteristic features of the culture system system. The first version of the model *2Dv.1* has been converted into a more detailed version, *2Dv.2*, which allows a more accurate description and analysis of processes such as synchronization, nutrient availability and merozoite spreading. Versions *2Dv.1* and *2Dv.2* provide compatible results, although some of the simulation parameters must be readjusted from version to version. Particularly, the values for P_{death} and P_{inf} are tuned when shifting from a version to the other.

Several aspects of the simulator can be improved. On the one hand, the individual model can be improved to account for different metabolites to better reproduce the limitations observed in closed culture systems. The biological complexity of the RBC is considerable, and the refinement of the individual model in this sense belongs to another kind of approach more oriented to the cellular level (i.e. whole cell models in System biology). On the other hand, such restrictions can be caused by the spatial structure of the system and the local environmental constraints on the infection process. The

approach in 2D does not allow for an accurate enough description of the local processes. A 3D model should be developed to better understand the spreading of the extracellular parasite and the limitations caused by the diffusion of substrate through the hematocrit layer. The aim of Chapter 3 is to analyse how the spatial structure of the culture at a system level affects these local processes, and consequently repercusses on the course of static *in vitro* cultures.